

Quantifying Privacy Leakage in Split Inference via Fisher-Approximated Shannon Information Analysis

Ruijun Deng^{1,2} Zhihui Lu^{1,3} Qiang Duan⁴

Abstract

Split inference (SI) partitions deep neural networks into distributed sub-models, enabling privacy-preserving collaborative learning. Nevertheless, it remains vulnerable to Data Reconstruction Attacks (DRAs), wherein adversaries exploit exposed smashed data to reconstruct raw inputs. Despite extensive research on adversarial attack-defense games, a shortfall remains in the fundamental analysis of privacy risks. This paper establishes a theoretical framework for privacy leakage quantification using information theory, defining it as the adversary’s certainty and deriving both average-case and worst-case error bounds. We introduce Fisher-approximated Shannon information (FSInfo), a novel privacy metric utilizing Fisher Information (FI) for operational privacy leakage computation. We empirically show that our privacy metric correlates well with empirical attacks and investigate some of the factors that affect privacy leakage, namely the data distribution, model size, and overfitting.

1. INTRODUCTION

Machine learning as a service (MLaaS) allows users to access machine learning (ML) services by simply uploading the raw data to be inferred. To enable privacy-preserving MLaaS, model partition, a mainstream research line of distributed machine learning, has been widely employed to segment deep neural networks (DNNs) into multiple sub-models and deploy them on different hosts (e.g., mobile phones and edge servers). These hosts conduct collaborative learning by communicating the data derived from the

¹School of Computer Science, Fudan University, Shanghai, China ²Engineering Research Center of Cyber Security Auditing and Monitoring, Ministry of Education, Shanghai, China ³Shanghai Blockchain Engineering Research Center, Shanghai, China. ⁴Information Sciences & Technology Department, Pennsylvania State University, Abington, PA, USA. Correspondence to: Zhihui Lu <lzh-fudan.edu.cn>, Ruijun Deng <rjdeng18-fudan.edu.cn>.

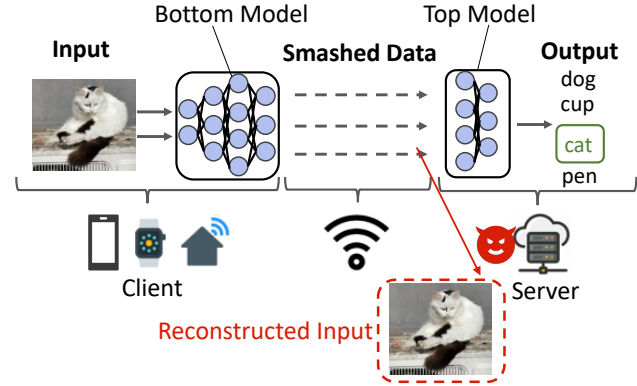


Figure 1. The information flow in a split inference system and the data reconstruction attack.

split layer (smashed data), thus hopefully preserving raw data privacy. This learning paradigm has been adopted in numerous model-distributed co-training and co-inference; for example, split/collaborative inference (SI) (Zhang et al., 2021; Li et al., 2021), split learning (SL) (Deng et al., 2023; Yu et al., 2024; Oh et al., 2022), vertical federated learning (VFL) (Chen et al., 2023), pipeline parallelism (Yuan et al., 2023; Ye et al., 2024), and their combinations (Duan et al., 2022). W.l.o.g, we focus on a two-party **split inference system** (see Figure 1) where the inputs are first fed into the bottom model on the client, and then the intermediate smashed data are transmitted to the top model on the server for further prediction, following Maeng et al. (Maeng et al., 2023) and Singh et al. (Singh et al., 2024). It is worth noting that this system represents each client-server pair in a multi-party distributed framework (e.g., VFL) and also corresponds to the forward computation in co-training (e.g., SL).

Despite transmitting only smashed data rather than raw inputs, the SI paradigm remains susceptible to privacy inference attacks. Adversaries can execute Membership Inference Attacks (MIAs) to identify training data participation (Song & Mittal, 2021; Wu et al., 2024), Attribute Inference Attacks (AIAs) to deduce sensitive attributes (e.g., demographic information) (Liu et al., 2022), and Data Reconstruction Attacks (DRAs) to recover original user data (He et al., 2019; Yang et al., 2022; Pasquini et al., 2021). Our research

focuses on DRAs due to their heightened severity: successful execution compromises entire datasets rather than isolated attributes, potentially causing substantial damage. As illustrated in Figure 1, the adversary (malicious server) can reconstruct input images after seeing the smashed data, demonstrating the critical nature of this vulnerability.

Privacy leakage quantification (or privacy quantification for short), is an independent concept that transcends the dualistic framework of privacy attack and defense. This critical but less investigated aspect of privacy issues on ML is to develop an appropriate measure (i.e., a privacy metric) of private information leakage from the exposed data (e.g., model parameters, gradients, and smashed data) about the raw input data. In this paper, privacy quantification means assessing the private information exposure from smashed data under DRAs in the SI system of Figure 1. The challenges for this can be presented through the lens of the twofold requirements: **i)** the privacy metric should be theoretically principled and possess a semantic interpretation aligned with privacy and security settings; and **ii)** the privacy metric should be quantitative and operationally computable, not just theoretical guidance.

Privacy quantification methods primarily fall into two categories: attack-based and theory-based approaches. Attack-based methods (Wu et al., 2024; Hu et al., 2023; Deng et al., 2023) measure privacy leakage through inference attacks, using success rates as empirical metrics. While operationally feasible, these methods rely heavily on adversary capabilities and provide only theoretical lower bounds without guarantees. Theory-based approaches employ various frameworks, including differential privacy (DP) (Singh et al., 2023), information theory (mutual information; MI) (Arevalo et al., 2024; Noorbakhsh et al., 2024), and hypothesis testing (Fisher information; FI) (Maeng et al., 2023). However, DP faces compatibility issues with nonlinear transformations in split inference, while MI often proves computationally intensive. Although FI offers theoretical rigor and computational efficiency, it focuses solely on mean squared error (MSE), limiting its privacy assessment scope. Consequently, existing methods exhibit inherent limitations in addressing these dual challenges simultaneously.

Contributions. In this paper, we tackle the two challenges by answering the following three questions: i) how to formulate privacy leakage theoretically; ii) how to easily compute the privacy leakage; and iii) what factors may potentially impact privacy leakage. For the first question, we formulate the privacy leakage as the certainty/confidence of the adversary with conditional entropy. Then, for the second question, we employ FI as a tool to directly calculate an approximation of defined privacy leakage, offering a quantitative and operational privacy metric called Fisher-approximated Shannon information (FSInfo) that also considers the adversary’s

Table 1. Comparisons of the privacy metrics.

Metrics	Bound	Comp.	Adv. Fea.	Adv. Err.
Attack		✓	✓	✓
Dcor		✓		
MI	✓			✓
FI	✓	✓	✓	
FSInfo	✓	✓	✓	✓

ability to exploit information. Finally, with FSInfo, we experimentally analyze the determinants of privacy leakage, including data distribution, model width and depth, and overfitting.

2. RELATED WORK

The privacy metrics (Wagner & Eckhoff, 2018) or privacy quantification, although having been studied decades ago in the areas of smart meter (Kalogridis et al., 2010) and database (Agrawal & Aggarwal, 2001), does not receive much attention in the field of machine learning until recently (Deng et al., 2024).

Current privacy metrics primarily emerge as byproducts of privacy attacks, demonstrating that attacks developed for breaching privacy can also be applied to quantify it (Wu et al., 2024; Hu et al., 2023; Deng et al., 2023; Abuadba et al., 2020; Pasquini et al., 2021; Liu et al., 2022). For instance, Liu et al. (Liu et al., 2022) developed the ML-Doctor framework, employing four distinct privacy inference attacks to assess private data and model parameter vulnerabilities. However, these empirical approaches, while intuitive, lack theoretical foundations and exhibit adversary-dependent limitations, potentially yielding overly optimistic privacy assessments with weaker adversaries (Deng et al., 2024).

Theoretical approaches offer deeper privacy analysis through advanced mathematical tools. Pan et al. (Pan et al., 2022) quantify privacy leakage via activated neuron counts, modeling it as a linear equation system’s complexity. However, this method primarily applies to fully connected networks (FCNs) with ReLU activations, limiting its effectiveness for nonlinear functions. While differential privacy (DP) remains a prominent DNN privacy framework, traditional local DP proves inadequate for both split inference and reconstruction attacks (Li et al., 2021; Singh et al., 2023; Tan et al., 2024). Singh et al. (Singh et al., 2023) address this limitation by generalizing DP to geodesic on the data manifold, yet DP’s inherent indistinguishability property, while effective against membership inference, demonstrates reduced efficiency and limited efficacy against reconstruction attacks, as empirically shown in (Tan et al., 2024).

Information-theoretic approaches, particularly Shannon mutual MI (Mireshghallah et al., 2020; Noorbakhsh et al., 2024; Arevalo et al., 2024) and distance correlation (Deng et al., 2024; Sun et al., 2022; 2021), quantify privacy leakage by measuring the information shared between A and B . Empirical studies demonstrate strong correlations between these metrics and adversarial recovery efficacy, including MSE and semantic similarity (Deng et al., 2024). Researchers have applied these measures to various data pairs: input features and smashed data (Mireshghallah et al., 2020; Noorbakhsh et al., 2024; Deng et al., 2024; Sun et al., 2021), training data and model parameters (Tan et al., 2024), and labels and smashed data (Sun et al., 2022). However, Shannon MI computation remains intractable for high-dimensional data (Arevalo et al., 2024), prompting recent approaches to circumvent direct calculation through noise injection (Tan et al., 2024) or adversarial learning (Noorbakhsh et al., 2024). Moreover, the previous MI-based privacy formulations neglect the characterization of the adversary.

FI metric (Hannun et al., 2021; Guo et al., 2022; Maeng et al., 2023), an easily computable privacy metric with a single backward pass, measures the error of the DRA adversary with theorems in hypothesis testing. However, they consider the mean squared error of the adversary as the privacy definition, which is only a specific part of the privacy.

As shown in Table 1, compared with the existing privacy metrics that can be adapted to the SI settings, FSInfo gives the theoretical lower bound on the adversary’s error (Bound) and is easily computable (Comp.). Also, its privacy leakage formulation considers the adversary’s power or the adversary’s feature of utilizing leaked information (Adv. Fea.) and is proved to have correlation with a general form of the adversary’s error function (Adv. Err).

3. PRELIMINARIES

3.1. Split Inference Pipeline

W.l.o.g, we consider a two-party split inference paradigm between the client D_1 and the server D_2 as shown in Figure 1. We focus on the privacy leakage from the smashed data of split inference about the raw input data. $\mathcal{U} = \{(x_i, y_i)_{i=1}^N \subseteq \mathbb{R}^{d_x} \times \mathbb{R}^{d_y}\}$ is a dataset corresponding to intelligent ML services. The two parties learn from \mathcal{U} with a split DNN $f_\theta(\cdot) = (f_{\theta_2} \circ f_{\theta_1})(\cdot) = f_{\theta_2}(f_{\theta_1}(\cdot))$, where D_1 holds the bottom model f_{θ_1} and D_2 the top model f_{θ_2} . The split point (SP) $p \in \{1, 2, \dots, L\}$ is the last layer of the bottom model f_{θ_1} , where L is the total number of layers of f_θ . The procedure starts with that D_1 takes as inputs a batch of raw data x^B and generates smashed data z^B as outputs; that is,

$$z^B = f_{\theta_1}(x^B), \quad (1)$$

where B is the batch size. Then, P_2 forwards z to get the predictions:

$$y^B = f_{\theta_2}(z^B). \quad (2)$$

For simplicity, we use x to denote a batch of raw data if there is no ambiguity.

3.2. Threat Model

We focus on the common setting of DRAs, where the mobile device with private data is benign and the edge server is untrusted.

Adversary’s Goal. In a data reconstruction attack (model inversion attack) (Yin et al., 2023; He et al., 2019), the goal of the adversary (edge server) \mathcal{A} is to reconstruct the value of raw data x :

$$\hat{x} = g_\phi(z), \quad (3)$$

where the g_ϕ is an attack function parameterized by ϕ , and \hat{x} is the reconstructed input.

Adversary’s Knowledge & Capability. As many DRAs rely on different prior knowledge to conduct reconstruction, less assumption about the adversary’s knowledge is preferred for broadening FSInfo’s applicability. Therefore, we do not leave tight requirements on the adversaries’ knowledge by allowing them to know and decide whether to use or not the plain-text smashed data z and all side information. i.e., the auxiliary dataset \mathcal{V} with the same distribution of \mathcal{U} , architecture and parameters of bottom model f_{θ_1} . This is compatible with most attacks (He et al., 2019; Yin et al., 2023; Yang et al., 2022) and the same as other privacy metrics (Maeng et al., 2023; Pasquini et al., 2021). For simplicity, we only consider the unbiased attack function g_ϕ , but one can apply our metric to the biased scenarios by using score matching techniques in (Maeng et al., 2023).

4. Privacy Leakage Quantification

4.1. Privacy and Privacy Leakage

The semantic meaning of privacy (information) depends on the diverse attributes of users and application contexts, e.g., culture and law. In contrast, privacy leakage, no matter what the privacy is (e.g., age or facial features), mainly depends on the ML task and threat model, i.e., the specific adversaries and their capabilities. For example, against the DRA adversaries in image classification tasks, privacy leakage is the value of training data x . Against MIA adversaries, privacy leakage is the membership of a single data x , i.e., the knowledge of whether or not x is used in training data of the model (Singh et al., 2023).

4.2. Privacy Leakage Formulation

In a SI system, we treat the raw input and the corresponding output of bottom model f_{θ_1} as two multi-dimensional random variables, X and Z , characterized by distributions $P(X)$ and $P(Z; X, \theta_1)$. After observing the Z , the adversary \mathcal{A} outputs the estimation \hat{X} of X . This process forms a Markov chain $X \rightarrow Z \rightarrow \hat{X}$.

In information theory, *entropy* $H(X)$ is a measure of the uncertainty of a random variable. Formally, we consider the privacy leakage as the certainty or confidence of \hat{X} given X as defined below:

Definition 4.1. (Privacy Leakage). Privacy Leakage about raw input data X from smashed data Z of model f_{θ_1} against adversary \mathcal{A} is the negative conditional entropy of the estimation \hat{X} given raw input data X :

$$\mathcal{L}_{f_{\theta_1}, X}^{\mathcal{A}} = -H(\hat{X}|X), \quad (4)$$

where \hat{X} is the reconstructed input of \mathcal{A} and a larger negative conditional entropy indicates more confident estimation \hat{X} given X and less error of the DRA adversary, thus larger privacy leakage.

We now give the relation between the $\mathcal{L}_{f_{\theta_1}, X}^{\mathcal{A}}$ and the average lower bound of the adversary's error:

Theorem 4.2. (Average-Case Reconstruction Error Bound). For two random variables raw input X and reconstructed input \hat{X} with the same dimension d_x , we have:

$$\frac{\mathbb{E}_{p(X, \hat{X})}[\|X - \hat{X}\|^2]}{d_x} \geq \frac{e^{\frac{2}{d_x} H(\hat{X}|X)}}{2\pi e}. \quad (5)$$

Theorem 4.2 indicates that the lower bound of the adversary's error is smaller under a higher privacy leakage.

Strongest Adversary (SA). Definition 4.1 captures the adversary's uncertainty of \hat{X} given X , serving as a naive criterion for measuring the recovery hardness. However, this definition remains agnostic to adversarial power, i.e., how accurate estimation the adversary can achieve. For instance, neural network (NN)-based adversary (He et al., 2019) typically achieve superior reconstruction accuracy compared to maximum likelihood estimation (MLE)-based approaches (He et al., 2019) as its $p(\hat{X})$ is closer to the $p(X)$ (He et al., 2019). To address this limitation, we extend the privacy leakage definition by incorporating adversarial power assumptions. We consider the "strongest" adversary as the one whose estimation \hat{X}^s has the least uncertainty among all possible estimators. This approach fundamentally differs from differential privacy's data-independent worst-case analysis, instead considering the adversarial worst-case across all potential attackers. Here, "strongest" specifically denotes reconstruction capability rather than knowledge or threat model characteristics.

Following this assumption, we introduce the definition of privacy leakage against the strongest adversary:

Definition 4.3. (Privacy Leakage against the SA). Privacy Leakage about raw input data X from smashed data Z of model f_{θ_1} against the strongest adversary \mathcal{A}^s is the negative conditional entropy of estimation \hat{X}^s given raw input data X :

$$\mathcal{L}_{f_{\theta_1}, X}^{\mathcal{A}^s} = -H(\hat{X}^s|X), \quad (6)$$

where \hat{X}^s is the reconstructed input of \mathcal{A}^s .

We then derive the relation between the privacy leakage definition in Definition 4.3 and the worst-case lower bound of the adversary's reconstruction error. We adopt the statistical minimax estimation setting (Scarlett & Cevher, 2019), to denote estimation loss as:

$$\ell(X, \hat{X}) = \Phi(\rho(X, \hat{X})), \quad (7)$$

where $\rho(X, \hat{X})$ is a metric and $\Phi(\cdot)$ is an increasing function maps from \mathbb{R}^+ to \mathbb{R}^+ . Equation 7 is a general formulation shared among many loss functions. For example, the MSE loss ($\ell(X, \hat{X}) = \frac{1}{d_x} \|X - \hat{X}\|_2^2$) used by (Maeng et al., 2023) as the privacy definition clearly takes this form (Scarlett & Cevher, 2019). The minimax risk of the adversary's estimation is

$$\mathcal{M}(\mathcal{X}, \ell) = \inf_{\hat{X} \in \hat{\mathcal{X}}} \sup_{X \in \mathcal{X}} \mathbb{E}_X[\ell(X, \hat{X})] \quad (8)$$

$$= \sup_{X \in \mathcal{X}} \mathbb{E}_X[\ell(X, \hat{X}^s)], \quad (9)$$

where \hat{X} are lie in subset $\hat{\mathcal{X}}$. $\mathcal{M}(\mathcal{X}, \ell)$ can be interpreted as the largest estimation error achieved by the strongest DRA adversary in this paper.

Then we can give the lower bound of the adversary's minimax risk with the variation of Fano inequality (Scarlett & Cevher, 2019) as:

Theorem 4.4. (Worst-Case Reconstruction Error Bound). Let random variables X , Z and \hat{X} form a Markov chain $X \rightarrow Z \rightarrow \hat{X}$ and X lie in the \mathcal{X} , such that

$$\rho(x_i, x_j) \geq \epsilon, \forall i, j \in \{1, \dots, |\mathcal{X}|\}, i \neq j. \quad (10)$$

Then, we have:

$$\mathcal{M}(\mathcal{X}, \ell) \geq \Phi\left(\frac{\epsilon}{2}\right) \left(1 - \frac{H(\hat{X}) - H(\hat{X}|X) + \log 2}{\log(|\mathcal{X}|)}\right), \quad (11)$$

where X is uniform over \mathcal{X} .

Due to space limitations, the proof for Theorem 4.2 and Theorem 4.4 is provided in the Appendix. Intuitively, this worst-case lower bound formally characterizes the quantitative relationship between privacy leakage (Definition 4.3) and the adversary's minimax risk, where ℓ represents a general loss

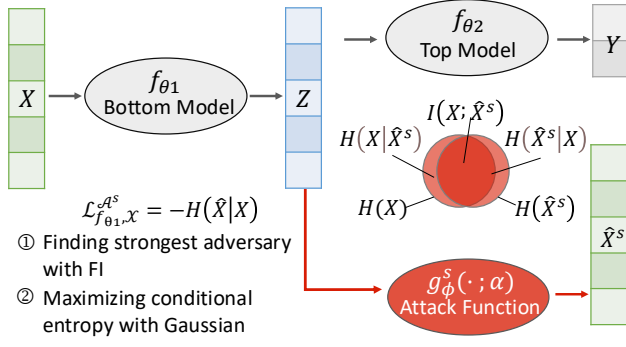


Figure 2. The proposed FSInfo privacy metric.

function adaptable to specific application scenarios. Specifically, increased privacy leakage $\mathcal{L}_{f_{\theta_1}, X}^{A^s} = -H(\hat{X}^s|X)$ directly corresponds to a lower minimax risk and less adversarial estimation error.

4.3. Computing Privacy Leakage

Definition 4.3 gives a privacy leakage definition as adversaries’ certainty. However, it can not be used directly for practitioners to evaluate the security level of a split inference framework, as the calculation of conditioned entropy or the MI of arbitrary high-dimensional random variables is a long-standing open problem (Noorbakhsh et al., 2024; Arevalo et al., 2024; Xiao & Devadas, 2023). Therefore, as shown in Figure 2, we translate Fisher information into a Shannon information quantity to estimate the certainty of the “strongest” adversary, i.e. $\mathcal{L}_{f_{\theta_1}, X}^{A^s}$. Then we use the Gaussian distribution to get maximum conditional entropy, offering an operational privacy metric, FSInfo.

Fisher information is a fundamental concept in statistics hypothesis testing (Martens, 2020), which is related to the asymptotic variability of an estimator, where higher FI means lower estimation error:

Definition 4.5. (Fisher Information Matrix) (Cover, 1999). For two random variables $x \sim p(x)$ and $z \sim p(z|x)$, the element of Fisher Information Matrix (FIM) or the Fisher Information (FI) $F_{z|x}$ of z w.r.t. the x is defined as:

$$\begin{aligned}
 F_{z|x}(i, j) &= \mathbb{E}_z \left[\left(\frac{\partial}{\partial x_i} \log p(z|x) \right) \left(\frac{\partial}{\partial x_j} \log p(z|x) \right) \right] \quad (12) \\
 &= -\mathbb{E}_z \left[\frac{\partial^2}{\partial x_i \partial x_j} \log p(z|x) \right], \quad (13)
 \end{aligned}$$

where the two formulations are equivalent (Martens, 2020) and $\log p(z|x)$ is the log conditional probability density function (p.d.f.) of z given x .

Note that, FI is defined based on the distribution; however, in the SI, the neural network f_{θ_1} is a deterministic function, and $p(z|x) = p(f_{\theta_1}(x)|x) = 1$. Therefore, we fit FI into SI

system by following (Maeng et al., 2023; Martens, 2020) which combine f_{θ_1} with a Gaussian distribution: $\hat{f}_{\theta_1}(\cdot) = r(f_{\theta_1}(\cdot))$, where $r(z) = z + \delta$, $\delta \sim \mathcal{N}(0, \sigma^2)$. To this end, we can calculate FI of raw input x contained by the smashed data z as:

$$F_{z|x} = \frac{1}{\sigma^2} J_{f_{\theta_1}}(x)^\top J_{f_{\theta_1}}(x), \quad (14)$$

where $J_{f_{\theta_1}}(x)$ is the Jacobian of z with respect to the raw input x .

The significance of FI is shown in the following theorem:

Theorem 4.6. (Cramér-Rao Bound) (Cover, 1999). The mean-squared error of any unbiased estimator $T(z)$ of the parameter x is lower bounded by the reciprocal of the Fisher information:

$$\text{Cov}(T) \geq F_{z|x}^{-1}, \quad (15)$$

where \geq is used in the Löwner partial order.

Cramér-Rao Bound gives the covariance’s lower bound of the estimator $T(z)$, or \hat{X} given $X = x$ in our DRA settings of SI, which can only be achieved by the “strongest” DRA adversary \mathcal{A}^s (see Section 4.2) who has the lowest estimation error. In other words, given $X = x$, the reconstructed distribution $p(\hat{X}^s|X = x)$ of the unbiased \mathcal{A}^s has a covariance of $\text{Cov}(\hat{X}^s) = F_{z|x}^{-1}$ and the mean of x .

Entropy Maximization. Among all the distributions with the same mean and covariance, the normal distribution $\mathcal{N}(x, F_{z|x}^{-1})$ maximizes entropy (Tan et al., 2024). To obtain the supremum of $H(\hat{X}^s|X = x)$ we let $p(\hat{X}^s|X = x) = \mathcal{N}(x, F_{z|x}^{-1})$ and further compute the $H(\hat{X}^s|X = x)$ as

$$H(\hat{X}^s|X = x) = \frac{1}{2} \log \left(\frac{(2\pi e)^{d_x}}{\det(F_{z|x})} \right), \quad (16)$$

where the d_x is the dimension of raw input x and $\det(F_{z|x})$ is the determinant of $F_{z|x}$.

Now, with the raw input X , we can directly calculate the approximation of privacy leakage against the strongest adversary \mathcal{A}^s in Definition 4.3 as:

$$\mathcal{L}_{f_{\theta_1}, X}^{A^s} = -H(\hat{X}^s|X) = -\mathbb{E}_{x \sim p(x)} \left[\frac{1}{2} \log \left(\frac{(2\pi e)^{d_x}}{\det(F_{z|x})} \right) \right], \quad (17)$$

where all the terms can be easily implemented.

Acceleration. The calculation of \mathcal{L}^{A^s} involves computing the Jacobian of z w.r.t. x , which is time-consuming when the d_x gets large (e.g., for a $32 \times 32 \times 3$ image in CIFAR10 (Krizhevsky et al., 2009), the number of rows of $F_{z|x}$ is 3072). We speed up this process by first approximating $F_{z|x}$

with its diagonal version, which is widely used in transfer learning (Fan et al., 2021; Xue et al., 2021):

$$\mathcal{L}_{f_{\theta_1, X}}^{\mathcal{A}^s} = -\frac{1}{2}\mathbb{E}_{x \sim p(X)}[d_x \log(2\pi e) - \log \det(F_{z|x})]. \quad (18)$$

Second, we use subsampling techniques such as average pooling to reduce input dimensions for image datasets.

Privacy Leakage per Dimension. Although $\mathcal{L}^{\mathcal{A}^s}$ can now outline the privacy leakage risk of an SI system, its value exhibits considerable variation w.r.t. the dimensionality of the input data, e.g., it tends to increase with the dimension of the input data. Therefore, we use the average FSInfo across all dimensions as a metric:

$$\overline{\mathcal{L}_{f_{\theta_1, X}}^{\mathcal{A}^s}} = \frac{\mathcal{L}_{f_{\theta_1, X}}^{\mathcal{A}^s}}{d_x}. \quad (19)$$

Definition 4.7. (FSInfo). In an SI system, the privacy metric FSInfo about X in the smashed data $Z = f_{\theta_1}(X)$ is:

$$FSInfo = \overline{\mathcal{L}_{f_{\theta_1, X}}^{\mathcal{A}^s}} \quad (20)$$

$$= -\frac{1}{2d_x}\mathbb{E}_{x \sim p(X)}[d_x \log(2\pi e) - \log \det(F_{z|x})]. \quad (21)$$

Definition 4.7 gives the essence link in DRA between the Fisher information and Shannon information, where the maximal Shannon information gain can be achieved by adversary \mathcal{A}^s whose estimation error is lower bounded by the Fisher information.

FSInfo serves as a crucial metric for both regulatory compliance and system optimization. From a regulatory perspective, it enables effective supervision of ML products, preventing market entry for systems with excessive privacy leakage risks. Adversaries can leverage FSInfo to identify vulnerable SI systems, optimizing their attack strategies, while practitioners can utilize it to select architectures and methodologies that minimize privacy leakage, thereby enhancing overall system security.

5. Experiments

In this section, we first apply our FSInfo on several models and datasets and compare it with other privacy metrics to validate the efficacy of FSInfo as a metric and demonstrate that privacy leakage is common in different settings. Second, we experimentally analyze factors that influence privacy leakage. We also provided results for privacy leakage for defenses SI systems in Appendix D.

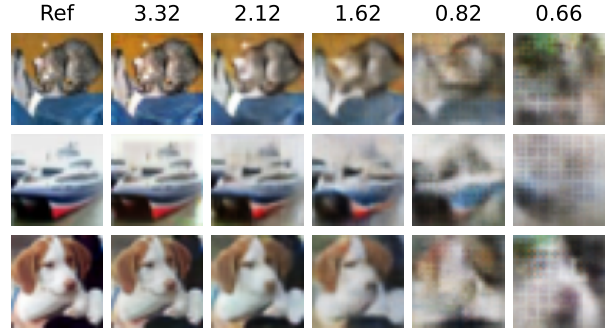


Figure 3. Visualization of raw input (left) and the reconstructed input of ResNet-18 on CIFAR-10 among different split points vs. their FSInfo.

5.1. Setups

5.1.1. DATASETS AND MODELS.

We follow the common settings of existing works on SI privacy attacks and defense (Yin et al., 2023; Noorbakhsh et al., 2024), where detailed dataset and model settings are provided in Appendix B. Image-based tasks are ubiquitous in ML applications, yet they present significant privacy concerns; hence, as a pioneering work, our first experimental study is primarily concentrated on image tasks. We use two datasets for our experiments: CIFAR-10 (Krizhevsky et al., 2009), and MNIST (LeCun et al., 1998). We use the train set for model training, and the test set for privacy metrics computing. We use four models including VGG-5 (Simonyan & Zisserman, 2014), VGG-9 (Simonyan & Zisserman, 2014), ResNet-18 (He et al., 2016), ResNet-34 (He et al., 2016). The number of critical layers and architecture of these models implemented for CIFAR-10 are presented in Appendix B. The split layer is identified by the index of that critical layer, starting from 1.

5.1.2. COMPARED METHODS AND METRICS

We empirically examined the FSInfo by comparing it with the three state-of-the-art (SOTA) methods: Diagonal Fisher information leakage (we use its reciprocal version: 1/dFIL) (Guo et al., 2022; Maeng et al., 2023), DLoss (Deng et al., 2024; Székely et al., 2007; Sun et al., 2021; 2022), and Mutual Information (MI) (Mireshghallah et al., 2020).

Unlike MIA settings where training data ratios in test sets provide measurable ground truth (Song & Mittal, 2021), there is no trivial way to experimentally control the ground truth privacy leakage due to the poor interpretability of neural networks (Deng et al., 2024). We therefore adopt reconstruction accuracy as our primary metric, aligning theoretical formulations with empirical observations. Following Section 3.2’s threat model, we adopt an NN-based DRA approach (He et al., 2019), as empirical evidence demon-

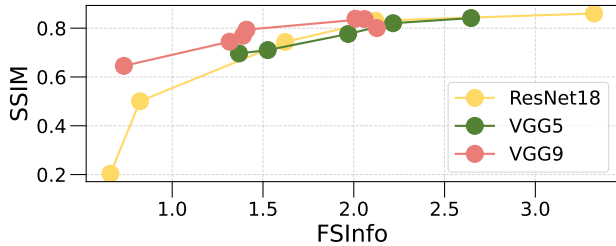


Figure 4. SSIM vs. FSInfo on three different models and CIFAR-10.

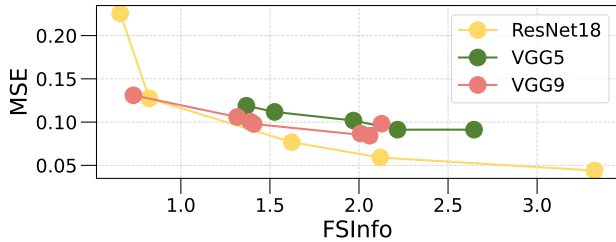


Figure 5. MSE vs. FSInfo on three different models and CIFAR-10.

strates superior reconstruction quality of NN-based methods compared to MLE-based approaches (Yin et al., 2023) (See Appendix A for detailed explanations). Evaluation incorporates standard DRA metrics: visual invertibility, Structural Similarity Index Measure (SSIM), and MSE. Note that these metrics only establish a lower bound for actual privacy leakage—at least what the attacker has already obtained has been leaked. The detailed introduction of the compared methods and metrics is given in Appendix C.

For comparison with SOTA privacy quantification methods with different value spans, inspired by Tan et al. (Tan et al., 2024), we construct the improvement criteria. Specifically, with privacy metrics denoted by $Metric$, the improvement (IMP) of compared methods and MSE is:

$$IMP(Metric) = (Metric_b - Metric) / Metric_b \quad (22)$$

$$IMP(MSE) = \left(\frac{1}{MSE_b} - \frac{1}{MSE} \right) / \frac{1}{MSE_b}, \quad (23)$$

where the experimental result with the highest degree of privacy leakage is designated with subscript b .

5.2. Validation of FSInfo

5.2.1. VALIDATION BY ATTACK SUCCESS METRICS

We first validate the efficacy of the FSInfo by comparing it with experimental DRA attack results. Figure 3 visualizes the raw input and the reconstructed image along with the averaged layer FSInfo. Generally, we observe that as the image clarity decreases, the corresponding FSInfo also decreases. **This indicates our FSInfo has a strong corre-**

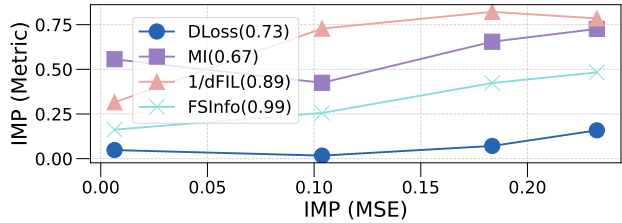


Figure 6. Evaluating different metrics in the Metric-MSE plane for four different split points of VGG-5 on CIFAR-10. We also report the Pearson correlation coefficient of each metric.

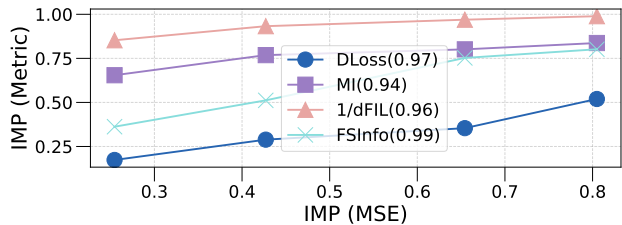


Figure 7. Evaluating different metrics in the Metric-MSE plane for four different split points of ResNet-18 on CIFAR-10. We also report the Pearson correlation coefficient of each metric.

lation with the visual quality of reconstructed images.

Then, we compare FSInfo in Figure 4 and Figure 5 with SSIM and MSE, two widely adopted objective metrics for DRA success. **First, We can see that FSInfo exhibits a positive correlation with SSIM and a negative correlation with MSE as expected, validating that the FSInfo reveals privacy leakage correctly.** Additionally, there is a rise in the line’s gradient of ResNet-18 when FSInfo approaches 0.5 in Figure 4. This demonstrates that chances are the adversary captures less privacy leakage than the actual extent, or the adversary’s capabilities are insufficient to exploit the full extent of the leaked privacy. This is also the reason for the downward trend of VGG-9’s line in Figure 4.

5.2.2. COMPARING WITH OTHER METHODS

Theoretically, FSInfo provides key theoretical advantages over alternatives: MI overlooks DRA-specific characteristics, while 1/dFIL’s MSE-only lower bound lacks generalizability. As demonstrated in Table 1 of the manuscript, FSInfo addresses both limitations.

However, experimentally, there is no ground truth for comparing the accuracy of different privacy metrics using diverse theoretical language to define privacy leakage, and thus, previous works like 1/dFIL (Guo et al., 2022) don’t compare their methods with others on the “accuracy” of quantified leakage. Instead, they only show that their metric is related to the attack success rate in the trend. Therefore, we compare our FSInfo with 1/dFIL, DLoss, and MI in the Metric-MSE plane and calculate their Pearson correla-

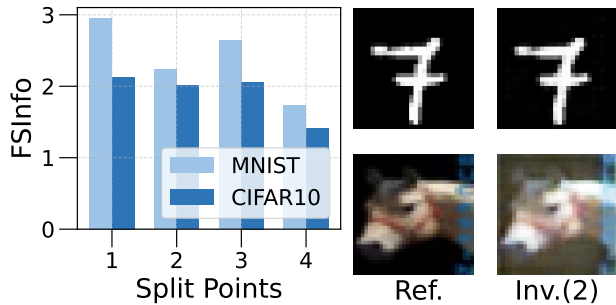


Figure 8. The impact of dataset complexity on privacy leakage. The left diagram is the FSInfo among different split layers of VGG-5 on MNIST and CIFAR-10. The right diagram is the raw inputs (Ref.) and the reconstructed inputs from split point 2 (Inv.(2)).

tion coefficients (PCC) to **showcase that the FSInfo has a stronger correlation with the changes of the adversary’s MSE**. As is shown in Figure 6 and Figure 7, the FSInfo achieves the best alignment with empirical observations among all metrics, whose PPC are both 0.99 on VGG-5 and ResNet-18. It also signifies that different privacy metrics themselves can disagree with each other on their way to approaching the ground-truth privacy leakage.

5.3. Factors Affecting Privacy Leakage

5.3.1. INTRINSIC DATA CHARACTERISTICS

CIFAR-10 comprises diverse RGB images across 10 classes, whereas MNIST contains grayscale handwritten digits. Normalized to $[-1, 1]$, CIFAR-10 exhibits richer pixel value diversity compared to MNIST’s bimodal distribution peaking at -1 and 1 (Appendix B). To investigate data characteristics’ impact on privacy leakage, we analyze FSInfo for both datasets on VGG-5 across four split points (Figure 8, left). Results demonstrate consistently lower privacy leakage for CIFAR-10, aligning with Liu et al.’s findings (Liu et al., 2022) that simpler images facilitate reconstruction. We attribute this discrepancy to dataset complexity and value space dimensions. Visual comparisons of raw and reconstructed images (Figure 8, right) reveal that MNIST adversaries primarily handle binary color patterns, while CIFAR-10 reconstruction requires capturing complex color distributions, suggesting that richer information content increases reconstruction difficulty.

5.3.2. MODEL WIDTH AND DEPTH

The model size (number of layers and the output size of a layer) influences neural network privacy characteristics. Figure 9 demonstrates that both reconstruction quality and FSInfo increase with channel size in ResNet-18, as wider networks exhibit more pronounced neuron activation patterns. Interestingly, the deeper network (ResNet-34) may

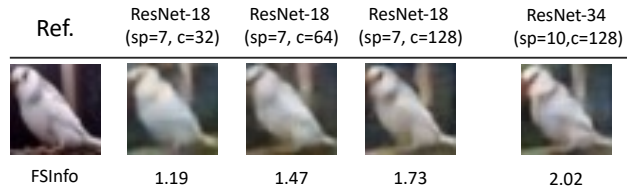


Figure 9. The impact of model size on privacy leakage on different models. Reconstructed inputs of the raw input (left) along with their FSInfo are displayed. The ResNet-18 architecture is displayed for three different base block channel sizes.

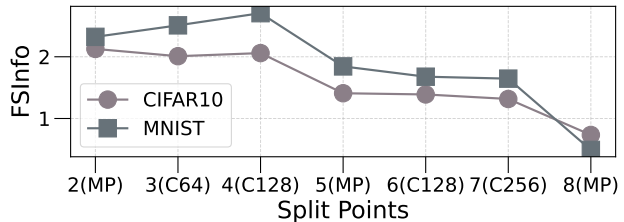


Figure 10. The impact of model size on privacy leakage on VGG-9 with different split points.

not always decrease the privacy leakage, because after being trained over 20 epochs, the ResNet-34 has a higher test accuracy than ResNet-18 on CIFAR-10, which may lead to a higher privacy leakage (see Section 5.3.3). Jiang et al. (Jiang et al., 2022) suggest that additional layers hinder leakage through increased transformations, which is consistent with the results of Figure 10 when SP is from 5 to 6. However, Figure 10 reveals this intuition may be incomplete, as later split points (e.g., SP is from 3 to 4) can exhibit greater leakage with increased width. Notably, at SP=8, MNIST shows lower leakage than CIFAR-10 due to MaxPooling’s differential impact on feature map dimensions ($7 \times 7 \rightarrow 3 \times 3$ vs. $8 \times 8 \rightarrow 4 \times 4$). Overall, network width substantially amplifies privacy leakage, while the increased depth degrades privacy leakage more moderately.

5.3.3. OVERFITTING

Following established methodologies (Liu et al., 2022; Song & Mittal, 2021; Carlini et al., 2019), we refer to the training epochs as the overfitting level. Figure 11 illustrates the relationship between epoch count and privacy leakage (FSInfo) for both VGG-5 and VGG-9, revealing a characteristic U-shaped pattern. Initially, untrained models exhibit high sensitivity to input stimuli, with a substantial gradient scale of smashed data w.r.t. the raw input responses leading to significant information leakage. As training progresses, this sensitivity gradually diminishes. However, prolonged training enables model parameters to memorize training data information, which subsequently manifests in smashed data during consequent testing (Achille et al., 2019), explaining the observed first-decline-then-rise FSInfo trajectory.

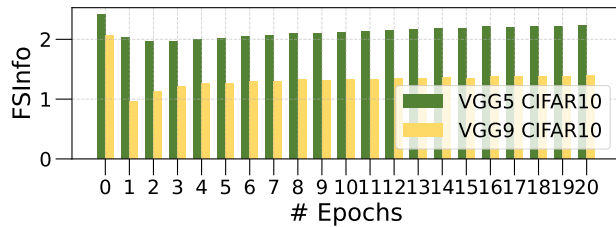


Figure 11. The impact of overfitting levels on privacy leakage. Epoch 0 means the model is just initialized and has not been trained.

6. Conclusion

We correlate the privacy leakage with the DRA adversary’s certainty and formulate it with conditional entropy, which can lower bound the adversary’s reconstruction error in both average- and worst-case. We obtain an operationally computable privacy metric, FSInfo, by transforming Fisher information into Shannon quantity. Experimental results showed that FSInfo aligns well with the human visual judgments on privacy leakage and the objective attack accuracy metrics. Also, we experimentally analyze factors that affect privacy leakage. Future work may extend the analysis of privacy leakage to more complex models (e.g., generative models) and other exposed information carriers (e.g., gradients in SL). Besides, the analysis of the privacy leakage determinants is conducted experimentally; future works may study theoretically and derive more interpretable results. Also, we experimentally analyze the determinants of privacy leakage.

References

- Abuadba, S., Kim, K., Kim, M., Thapa, C., Camtepe, S. A., Gao, Y., Kim, H., and Nepal, S. Can we use split learning on 1d cnn models for privacy preserving training? In *Proceedings of the 15th ACM Asia Conference on Computer and Communications Security*, pp. 305–318, New York, NY, USA, 2020. Association for Computing Machinery.
- Achille, A., Paolini, G., and Soatto, S. Where is the information in a deep neural network? *arXiv preprint arXiv:1905.12213*, 2019.
- Agrawal, D. and Aggarwal, C. C. On the design and quantification of privacy preserving data mining algorithms. In *Proceedings of the twentieth ACM SIGMOD-SIGACT-SIGART symposium on Principles of database systems*, pp. 247–255, New York, NY, USA, 2001. Association for Computing Machinery.
- Arevalo, C. A., Noorbakhsh, S. L., Dong, Y., Hong, Y., and Wang, B. Task-agnostic privacy-preserving representation learning for federated learning against attribute inference attacks. In *Proceedings of the AAAI Conference on Artificial Intelligence*, volume 38, pp. 10909–10917, 2024.
- Carlini, N., Liu, C., Erlingsson, Ú., Kos, J., and Song, D. The secret sharer: Evaluating and testing unintended memorization in neural networks. In *28th USENIX Security Symposium (USENIX Security 19)*, pp. 267–284, Santa Clara, CA, 2019. USENIX Association.
- Chen, P., Yang, J., Lin, J., Lu, Z., Duan, Q., and Chai, H. A practical clean-label backdoor attack with limited information in vertical federated learning. In *2023 IEEE International Conference on Data Mining (ICDM)*, pp. 41–50. IEEE, 2023.
- Cover, T. M. *Elements of information theory*. John Wiley & Sons, 1999.
- Deng, R., Du, X., Lu, Z., Duan, Q., Huang, S.-C., and Wu, J. Hsfl: Efficient and privacy-preserving offloading for split and federated learning in iot services. In *2023 IEEE International Conference on Web Services (ICWS)*, pp. 658–668. IEEE, 2023.
- Deng, R., Hu, S., Lin, J., Yang, J., Lu, Z., Wu, J., Huang, S.-C., and Duan, Q. Invmetrics: Measuring privacy risks for split model-based customer behavior analysis. *IEEE Transactions on Consumer Electronics*, 70(1):4168–4177, 2024.
- Duan, Q., Hu, S., Deng, R., and Lu, Z. Combined federated and split learning in edge computing for ubiquitous intelligence in internet of things: State-of-the-art and future directions. *Sensors*, 22(16):5983, 2022.
- Fan, Z., Shi, L., Liu, Q., Li, Z., and Zhang, Z. Discriminative fisher embedding dictionary transfer learning for object recognition. *IEEE Transactions on Neural Networks and Learning Systems*, 34(1):64–78, 2021.
- Geiping, J., Bauermeister, H., Dröge, H., and Moeller, M. Inverting gradients-how easy is it to break privacy in federated learning? *Advances in neural information processing systems*, 33:16937–16947, 2020.
- Ghosh, S., Liao, Q. V., Ramamurthy, K. N., Navratil, J., Sattigeri, P., Varshney, K. R., and Zhang, Y. Uncertainty quantification 360: A holistic toolkit for quantifying and communicating the uncertainty of ai, 2021.
- Guo, C., Karrer, B., Chaudhuri, K., and van der Maaten, L. Bounding training data reconstruction in private (deep) learning. In *International Conference on Machine Learning*, pp. 8056–8071. PMLR, 2022.
- Hannun, A., Guo, C., and van der Maaten, L. Measuring data leakage in machine-learning models with fisher information. In *Uncertainty in Artificial Intelligence*, pp. 760–770. PMLR, 2021.

- He, K., Zhang, X., Ren, S., and Sun, J. Deep residual learning for image recognition. In *Proceedings of the IEEE conference on computer vision and pattern recognition*, pp. 770–778, 2016.
- He, Z., Zhang, T., and Lee, R. B. Model inversion attacks against collaborative inference. In *Proceedings of the 35th Annual Computer Security Applications Conference*, pp. 148–162, New York, NY, USA, 2019. Association for Computing Machinery.
- Hu, Y., Liang, W., Wu, R., Xiao, K., Wang, W., Li, X., Liu, J., and Qin, Z. Quantifying and defending against privacy threats on federated knowledge graph embedding. In *Proceedings of the ACM Web Conference 2023*, pp. 2306–2317, New York, NY, USA, 2023. Association for Computing Machinery.
- Jiang, H., Liu, M., Sun, S., Wang, Y., and Guo, X. Fedstyl: Computation-efficient federated synergy learning on heterogeneous iot devices. In *2022 IEEE/ACM 30th International Symposium on Quality of Service (IWQoS)*, pp. 1–10. IEEE, 2022.
- Jin, X., Chen, P.-Y., Hsu, C.-Y., Yu, C.-M., and Chen, T. Cafe: Catastrophic data leakage in vertical federated learning. *Advances in Neural Information Processing Systems*, 34:994–1006, 2021.
- Kalogridis, G., Efthymiou, C., Denic, S. Z., Lewis, T. A., and Cepeda, R. Privacy for smart meters: Towards undetectable appliance load signatures. In *2010 first IEEE international conference on smart grid communications*, pp. 232–237. IEEE, 2010.
- Krizhevsky, A., Hinton, G., et al. Learning multiple layers of features from tiny images. 2009.
- LeCun, Y., Bottou, L., Bengio, Y., and Haffner, P. Gradient-based learning applied to document recognition. *Proceedings of the IEEE*, 86(11):2278–2324, 1998.
- Li, O., Sun, J., Yang, X., Gao, W., Zhang, H., Xie, J., Smith, V., and Wang, C. Label leakage and protection in two-party split learning. In *International Conference on Learning Representations*, 2021.
- Liu, Y., Wen, R., He, X., Salem, A., Zhang, Z., Backes, M., De Cristofaro, E., Fritz, M., and Zhang, Y. {ML-Doctor}: Holistic risk assessment of inference attacks against machine learning models. In *31st USENIX Security Symposium (USENIX Security 22)*, pp. 4525–4542, Boston, MA, 2022. USENIX Association.
- Maeng, K., Guo, C., Kariyappa, S., and Suh, E. Measuring and controlling split layer privacy leakage using fisher information. In *Workshop on Federated Learning: Recent Advances and New Challenges (in Conjunction with NeurIPS 2022)*.
- Maeng, K., Guo, C., Kariyappa, S., and Suh, G. E. Bounding the invertibility of privacy-preserving instance encoding using fisher information. *Advances in Neural Information Processing Systems*, 36:51904–51925, 2023.
- Martens, J. New insights and perspectives on the natural gradient method. *Journal of Machine Learning Research*, 21(146):1–76, 2020.
- Mireshghallah, F., Taram, M., Ramrakhiani, P., Jalali, A., Tullsen, D., and Esmaeilzadeh, H. Shredder: Learning noise distributions to protect inference privacy. In *Proceedings of the Twenty-Fifth International Conference on Architectural Support for Programming Languages and Operating Systems*, pp. 3–18, New York, NY, USA, 2020. Association for Computing Machinery.
- Noorbakhsh, S. L., Zhang, B., Hong, Y., and Wang, B. {Inf2Guard}: An {Information-Theoretic} framework for learning {Privacy-Preserving} representations against inference attacks. In *33rd USENIX Security Symposium (USENIX Security 24)*, pp. 2405–2422, Philadelphia, PA, 2024. USENIX Association.
- Oh, S., Park, J., Vepakomma, P., Baek, S., Raskar, R., Benis, M., and Kim, S.-L. Locfedmix-sl: Localize, federate, and mix for improved scalability, convergence, and latency in split learning. In *Proceedings of the ACM Web Conference 2022*, pp. 3347–3357, New York, NY, USA, 2022. Association for Computing Machinery.
- Pan, X., Zhang, M., Yan, Y., Zhu, J., and Yang, Z. Exploring the security boundary of data reconstruction via neuron exclusivity analysis. In *31st USENIX Security Symposium (USENIX Security 22)*, pp. 3989–4006, Boston, MA, 2022. USENIX Association.
- Pasquini, D., Ateniese, G., and Bernaschi, M. Unleashing the tiger: Inference attacks on split learning. In *Proceedings of the 2021 ACM SIGSAC Conference on Computer and Communications Security*, pp. 2113–2129, New York, NY, USA, 2021. Association for Computing Machinery.
- Scarlett, J. and Cevher, V. An introductory guide to fano’s inequality with applications in statistical estimation. *arXiv preprint arXiv:1901.00555*, 2019.
- Shwartz-Ziv, R. and Tishby, N. Opening the black box of deep neural networks via information. *arXiv preprint arXiv:1703.00810*, 2017.
- Simonyan, K. and Zisserman, A. Very deep convolutional networks for large-scale image recognition. *arXiv preprint arXiv:1409.1556*, 2014.
- Singh, A., Vepakomma, P., Sharma, V., and Raskar, R. Posthoc privacy guarantees for collaborative inference with modified propose-test-release. *Advances in Neural Information Processing Systems*, 36:26438–26451, 2023.

- Singh, A., Sharma, V., Sukumaran, R., Mose, J., Chiu, J., Yu, J., and Raskar, R. Simba: Split inference—mechanisms, benchmarks and attacks. In *European Conference on Computer Vision*, pp. 214–232. Springer, 2024.
- Song, L. and Mittal, P. Systematic evaluation of privacy risks of machine learning models. In *30th USENIX Security Symposium (USENIX Security 21)*, pp. 2615–2632. USENIX Association, 2021.
- Sun, J., Yao, Y., Gao, W., Xie, J., and Wang, C. Defending against reconstruction attack in vertical federated learning. *arXiv preprint arXiv:2107.09898*, 2021.
- Sun, J., Yang, X., Yao, Y., and Wang, C. Label leakage and protection from forward embedding in vertical federated learning. *arXiv preprint arXiv:2203.01451*, 2022.
- Sun, X., Gazagnadou, N., Sharma, V., Lyu, L., Li, H., and Zheng, L. Privacy assessment on reconstructed images: are existing evaluation metrics faithful to human perception? *Advances in Neural Information Processing Systems*, 36:10223–10237, 2024.
- Székely, G. J., Rizzo, M. L., and Bakirov, N. K. Measuring and testing dependence by correlation of distances. *The Annals of Statistics*, 35(6):2769 – 2794, 2007.
- Tan, Q., Li, Q., Zhao, Y., Liu, Z., Guo, X., and Xu, K. Defending against data reconstruction attacks in federated learning: An information theory approach. In *33rd USENIX Security Symposium (USENIX Security 24)*, pp. 325–342, Philadelphia, PA, 2024. USENIX Association.
- Tishby, N. and Zaslavsky, N. Deep learning and the information bottleneck principle. In *2015 IEEE information theory workshop (itw)*, pp. 1–5. IEEE, 2015.
- Vepakomma, P., Singh, A., Gupta, O., and Raskar, R. Nopeek: Information leakage reduction to share activations in distributed deep learning. In *2020 International Conference on Data Mining Workshops (ICDMW)*, pp. 933–942. IEEE, 2020.
- Wagner, I. and Eckhoff, D. Technical privacy metrics: a systematic survey. *ACM Computing Surveys (CSUR)*, 51(3):1–38, 2018.
- Wu, Y., Wen, R., Backes, M., Berrang, P., Humbert, M., Shen, Y., and Zhang, Y. Quantifying privacy risks of prompts in visual prompt learning. pp. 5841–5858, 2024.
- Xiao, H. and Devadas, S. Pac privacy: Automatic privacy measurement and control of data processing. In *Annual International Cryptology Conference*, pp. 611–644. Springer, 2023.
- Xue, Y., Niu, C., Zheng, Z., Tang, S., Lyu, C., Wu, F., and Chen, G. Toward understanding the influence of individual clients in federated learning. In *Proceedings of the AAAI Conference on Artificial Intelligence*, volume 35, pp. 10560–10567, 2021.
- Yang, M., Li, Z., Wang, J., Hu, H., Ren, A., Xu, X., and Yi, W. Measuring data reconstruction defenses in collaborative inference systems. *Advances in Neural Information Processing Systems*, 35:12855–12867, 2022.
- Ye, S., Du, J., Zeng, L., Ou, W., Chu, X., Lu, Y., and Chen, X. Galaxy: A resource-efficient collaborative edge ai system for in-situ transformer inference. In *IEEE INFOCOM 2024 - IEEE Conference on Computer Communications*, pp. 1001–1010, 2024. doi: 10.1109/INFOCOM52122.2024.10621342.
- Yin, Y., Zhang, X., Zhang, H., Li, F., Yu, Y., Cheng, X., and Hu, P. Ginver: Generative model inversion attacks against collaborative inference. In *Proceedings of the ACM Web Conference 2023*, pp. 2122–2131, New York, NY, USA, 2023. Association for Computing Machinery.
- Yu, D., Du, X., Jiang, L., Tong, W., and Deng, S. Ecsnn: Splitting deep spiking neural networks for edge devices. In Larson, K. (ed.), *Proceedings of the Thirty-Third International Joint Conference on Artificial Intelligence, IJCAI-24*, pp. 5389–5397. International Joint Conferences on Artificial Intelligence Organization, 8 2024. doi: 10.24963/ijcai.2024/596. URL <https://doi.org/10.24963/ijcai.2024/596>. Main Track.
- Yu, S., Wickstrøm, K., Jenssen, R., and Principe, J. C. Understanding convolutional neural networks with information theory: An initial exploration. *IEEE transactions on neural networks and learning systems*, 32(1):435–442, 2020.
- Yuan, L., He, Q., Chen, F., Dou, R., Jin, H., and Yang, Y. Pipeedge: A trusted pipelining collaborative edge training based on blockchain. In *Proceedings of the ACM Web Conference 2023*, pp. 3033–3043, New York, NY, USA, 2023. Association for Computing Machinery.
- Zhang, L., Chen, L., and Xu, J. Autodidactic neurosurgeon: Collaborative deep inference for mobile edge intelligence via online learning. In *Proceedings of the Web Conference 2021*, pp. 3111–3123, New York, NY, USA, 2021. Association for Computing Machinery.
- Zhang, R., Guo, S., Wang, J., Xie, X., and Tao, D. A survey on gradient inversion: Attacks, defenses and future directions. In *Proceedings of the Thirty-First International Joint Conference on Artificial Intelligence*, pp. 5678–685, 2023.

A. More Related Work

A.1. Data Reconstruction Attacks to SI

Discriminative Reconstruction Attacks (DRAs) employ two primary approaches: neural network (NN)-based methods, which learn mappings from observable outputs to raw inputs, and maximum likelihood estimation (MLE)-based methods, utilizing optimization techniques like stochastic gradient descent (He et al., 2019). In federated learning, where only aggregated parameters and gradients are observable, MLE-based methods dominate, typically optimizing gradient matching objectives (euclidean or cosine similarity) (Zhang et al., 2023; Geiping et al., 2020; Jin et al., 2021).

SI scenarios favor NN-based methods due to the direct one-to-one correspondence between raw inputs and smashed data, providing ample training pairs for inverse neural networks (Yin et al., 2023; Pasquini et al., 2021). Recent SI-focused DRA research primarily enhances attack accuracy under constrained conditions, such as lacking auxiliary datasets (Yin et al., 2023) or facing defense mechanisms (Yang et al., 2022). Empirical evidence demonstrates superior reconstruction quality of NN-based methods compared to MLE-based approaches (Yin et al., 2023).

A.2. Information in Deep Neural Network

In the information theory, *entropy* $H(X)$ is a measure of the uncertainty of a random variable X and (Shannon) mutual information $I(X; Y)$ between random variables X and Y is the reduction in the uncertainty of X due to the knowledge of Y , and vice versa (Cover, 1999):

$$I(X; Y) = H(X) - H(X|Y) = H(Y) - H(Y|X). \quad (24)$$

Previous studies (Tishby & Zaslavsky, 2015; Yu et al., 2020) analyze DNNs by seeing the inputs, predictions, and outputs of one hidden layer (representations) as random variables X , Y , and Z . Model optimization can be done by minimizing $I(X; Z)$ and maximizing $I(Z; Y)$ under the information bottleneck (IB) tradeoff (Shwartz-Ziv & Tishby, 2017; Yu et al., 2020).

B. Experimental Implementations

B.1. Implementation

Our experiments were performed on a server equipped with two NVIDIA Geforce RTX 4090 24GB GPUs, two Intel Xeon Silver 4310 CPUs, and 256GB of memory. We implemented the proposed metric with Python 3.8.13, and Pytorch 1.12.1.

B.2. Datasets

Table 2. Statistics of Datasets

Dataset	# Train	# Test	# Feature	# Class
CIFAR-10	50,000	10,000	32x32x3	10
MNIST	60,000	10,000	28x28x1	10

We evaluated our metrics on four tasks with two real-world datasets (CIFAR-10 (Krizhevsky et al., 2009) and MNIST (LeCun et al., 1998)) as shown in Table 2. Both datasets are normalized into $[-1, 1]$.

CIFAR10 (Krizhevsky et al., 2009): Comprising 50,000 training samples and 10,000 test samples across 10 classes, **CIFAR-10** dataset is a benchmark in computer vision with categories like airplanes, automobiles, and birds. Each image is a 32x32 pixel color image with three channels.

MNIST (LeCun et al., 1998): Comprising 60,000 training samples and 10,000 test samples across 10 digits, with each image being a 28x28 gray-scale image.

Figure 12 plots the distribution of the first image of CIFAR-10 and MNIST respectively. We bin the continuous pixel value of two images into 100 (for CIFAR-10) and 10 (for MNIST) discrete intervals between -1 and 1.

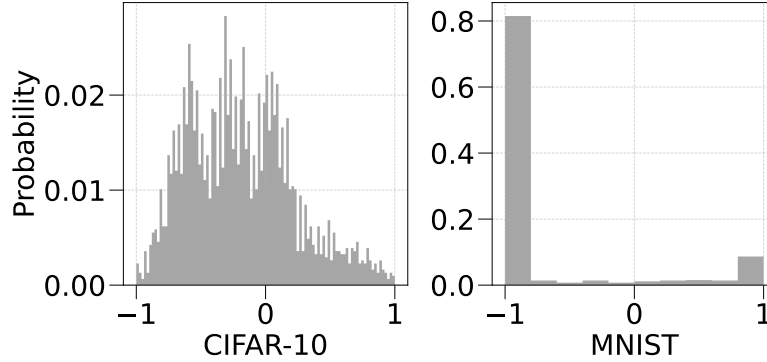


Figure 12. The distribution of the first image of CIFAR-10 and MNIST datasets.

Table 3. Statistics of Models. Convolution layers are denoted by C, followed by the number of filters; MaxPooling, AveragePooling, and Adaptive AveragePooling layers are MP, AP, and AAP; Fully Connected layer is FC with the number of neurons; Basic Block of ResNet is BB with the channel size.

Model	# Critical Layer	Architecture
VGG-5	7	C32-MP-C64(default)-MP-C64-FC128-FC10
VGG-9	14	C64-MP-C64-C128-MP(default)-C128-C256-MP-C256-MP-C256-FC4096-FC10
ResNet-18	12	C64-AP-[BB64]*2-[BB128]*2 (default)-[BB256]*2-[BB512]*2-AAP-FC10
ResNet-34	20	C64-AP-[BB64]*3-[BB128]*4 (default)-[BB256]*6-[BB512]*3-AAP-FC10

B.3. Models

We use four models including VGG-5 (Simonyan & Zisserman, 2014), VGG-9 (Simonyan & Zisserman, 2014), ResNet-18 (He et al., 2016), ResNet-34 (He et al., 2016), as shown in Table. 3.

The number of critical layers and architecture of these models implemented for CIFAR-10 are presented in Table 3. We also identify the default split layer in the brackets. All models are trained until the test accuracy tends to stabilize by default (approximately 20 epochs). The Gaussian distribution for initialize the parameters of f_{θ_1} is $\mathcal{N}(0, 0.01)$.

C. Details of Compared Methods and Metrics

C.1. Compared Methods

Diagonal Fisher information leakage (dFIL) (Guo et al., 2022; Maeng et al., 2023) views the DRA as parameter estimation and utilizes Fisher information to bound the estimation error as follows:

$$\mathbb{E}[\|\hat{x} - x\|_2^2/d] \geq \frac{1}{dFIL} \quad (25)$$

$$dFIL = Tr(\mathcal{I}_z(x))/d, \quad (26)$$

where the dimension of input x is d , $Tr(\cdot)$ denotes the matrix trace, \hat{x} is the reconstructed input, and $\mathcal{I}(\cdot)$ is the Fisher information matrix of smashed data z with respect to x . Following Maeng et al.(Maeng et al., 2023), we use the reciprocal of dFIL ($1/dFIL$), the high value of which indicates less privacy leakage.

DLoss (Deng et al., 2024; Székely et al., 2007; Sun et al., 2021; 2022) calculates the privacy leakage as the distance correlation between raw input X and smashed data Z , which can measure the nonlinear dependence between these random

vectors:

$$\begin{aligned} \text{DLoss}(X, Z) &= \sqrt{\mathcal{R}^2(X, Z)}, \\ \text{s.t. } X_i &\sim p(X), Z_i \sim q(X), i = 1, \dots, b, \end{aligned} \tag{27}$$

where the $\mathcal{R}^2(X, Z)$ is the distance covariance between X and Z .

Mutual Information (MI) (Mireshghallah et al., 2020) calculates the privacy leakage as the Shannon mutual information using the Information Theoretical Estimators Toolbox (Ghosh et al., 2021) as:

$$\text{MI}(x, z) = \int_x \int_z p_{x,z} \log \frac{p_{x,z}}{p_x p_z} dx dz, \tag{28}$$

where x and z are the raw input and smashed data.

C.2. Metrics

Visual invertibility measures the similarity of the raw input and the reconstructed one by human perception (Sun et al., 2024). We visualize the reconstructed images and observe their clarity and similarity to the raw input. This metric offers semantic judgment for privacy information observed by the adversary. A higher visual quality means a larger privacy leakage.

SSIM is an objective criterion for measuring the pixel-wise similarity of two images with values ranging from 0 to 1. A higher SSIM means a larger privacy leakage.

MSE is also an objective criterion, which measures the error or distance between two images. A large MSE indicates less privacy leakage.

D. Examining Defense mechanisms

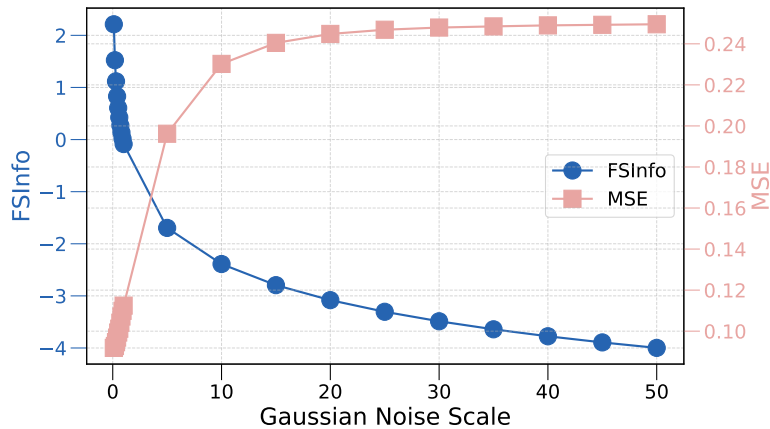


Figure 13. Changing trend of FSInfo and MSE with the growth of Gaussian noise scale on VGG-5.

As mentioned in Section 4.3, as a privacy metric, FSInfo can be used for analyzing and supervising the privacy risks of DNN-based products. In this section, we experimentally validate that, practitioners can also use FSInfo to assess the split inference system employed defense mechanisms, demonstrating the practical relevance of our study.

The unique characteristics of split inference necessitate distinct privacy protection approaches compared to traditional federated learning. In split inference, the smashed data maintains a one-to-one correspondence with the raw input, rather than representing an aggregated form of the raw input. Consequently, the batch size, which often serves as a privacy consideration in federated learning, may not significantly affect privacy leakage in the smashed data of split inference (Geiping et al., 2020). This characteristic also explains why standard DP is unsuitable for split learning scenarios—the standard DP definition of neighboring databases requires that outputs for any two samples remain nearly indistinguishable, regardless of their differences (Singh et al., 2023). Consequently, obfuscation-based defense mechanisms, particularly those utilizing direct noise injection or adversarial representation learning techniques, have become predominant in split inference systems (Singh et al., 2024).

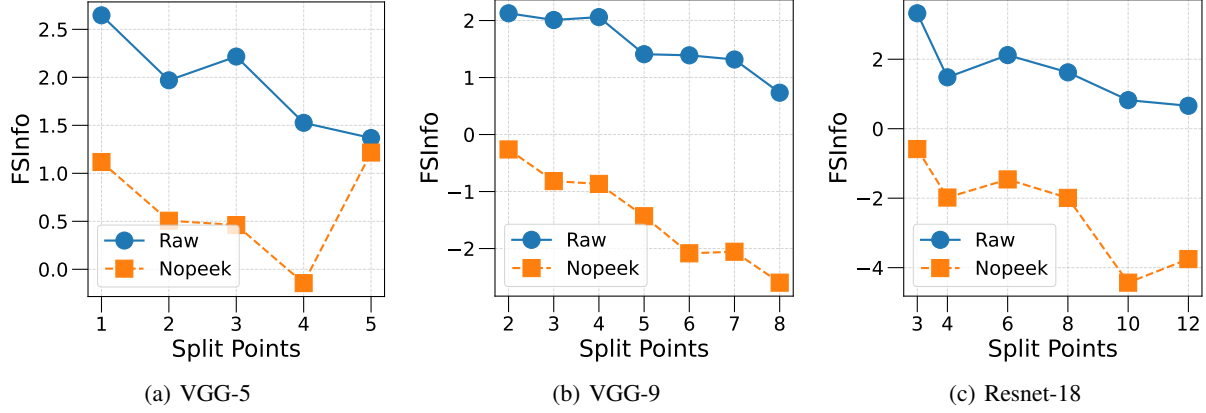


Figure 14. FSInfo under Nopeek defense mechanisms on CIFAR-10.

We apply the proposed FSInfo framework to split inference systems incorporating these two obfuscation defense mechanisms:

- Gaussian noise (Singh et al., 2024) directly adds noise from Gaussian distribution on the raw smashed data before sending it to the server.
- Nopeek (Vepakomma et al., 2020) uses adversarial representation learning methods in the model training phase to guide the bottom model to output smashed data with less information of raw input. For raw input data X , smashed data Z , true labels Y_{true} and predicted labels Y , the loss function of Nopeek is:

$$\alpha_1 DLoss(X, Z) + \alpha_2 CCE(Y_{true}, Y),$$

where the $DLoss$ is the privacy metric mentioned in Section 5.1.2, and the CCE is the cross-entropy loss function.

Figure 13 shows the changing trend of FSInfo and MSE with the growth of Gaussian noise scale on VGG-5 (with the default split layer mentioned in Section 6 in the paper) and CIFAR-10, where we varied the Gaussian noise from 0.1 to 50. As we can tell, **FSInfo thinks an SL system with higher defense strength (higher noise scale) may leak less leakage.**

We train the VGG-5, VGG-9, and ResNet-18 with Nopeek on CIFAR-10 to get the protected model, where both α_1 and α_2 are 0.5. Figure 14 shows the FSInfo on different split points on both raw and protected models. The results demonstrate that **after defense, the smashed data leaks less information about the raw input.** Also, Figure 14 (a) shows that privacy leakage of the 5-th split point (the first fully connected layer of VGG-5) of the protected model is larger than that of the 4-th, indicating that Nopeek **may be less effective for defending privacy leakage from the first fully connected layer after the convolutional layers.**

E. Proof of Theorem 4.2

Tan et al. (Tan et al., 2024) have modeled the estimation error of the DRA adversaries who aim at reconstructing the training dataset $D \in \mathbb{R}^d$ of one client from the model parameters $W \in \mathbb{R}^m$ in the federated learning scenarios by giving Theorem 1 in (Tan et al., 2024):

Theorem E.1. (Theorem 1 in (Tan et al., 2024)). For any random variable $D \in \mathbb{R}^d$ and $W \in \mathbb{R}^m$, we have

$$\mathbb{E}[\|D - \hat{D}(W)\|^2/d] \geq \frac{e^{2h(D)/d}}{2\pi e} e^{-2I(D;W)/d}, \quad (29)$$

where $\hat{D}(W)$ is an estimator of D constructed by W .

By simply applying Theorem E.1 in the privacy quantification in smashed data about raw input in split inference settings, we reach Theorem 4.2. For better understanding, we follow (Tan et al., 2024) to give the proof details of Theorem 4.2 as follows:

To prove Theorem 4.2, we first introduce the following lemma:

Lemma E.2. (Lemma 2 in (Tan et al., 2024)). For any d_x -dimensional semi-positive definite matrix A ($A \in \mathbb{R}^{d_x \times d_x}$), we have:

$$\det(A) \leq \left(\frac{\text{tr}(A)}{d_x}\right)^{d_x}, \quad (30)$$

where the $\det(\cdot)$ is the determinant and the $\text{tr}(\cdot)$ denotes the trace.

Now, we prove the Theorem 4.2 as below:

Proof. Let X be the raw input and \hat{X} be the reconstructed input, we have:

$$H(\hat{X}|X) \quad (31)$$

$$= \mathbb{E}_{x \sim p(X)} H(\hat{X}|X = x) \quad (32)$$

$$\leq \mathbb{E}_{x \sim p(X)} \left[\frac{d_x}{2} \log(2\pi e) + \frac{1}{2} \log \det(\text{Cov}(\hat{X}|X = x)) \right] \quad (33)$$

$$= \frac{d_x}{2} \log(2\pi e) + \mathbb{E}_{x \sim p(X)} \left[\frac{1}{2} \log \det(\text{Cov}(\hat{X}|X = x)) \right] \quad (34)$$

$$\leq \frac{d_x}{2} \log(2\pi e) + \mathbb{E}_{x \sim p(X)} \left[\frac{d_x}{2} \log \frac{\text{tr}(\text{Cov}(\hat{X}|X = x))}{d_x} \right] \quad (35)$$

$$= \frac{d_x}{2} \log(2\pi e) + \mathbb{E}_{x \sim p(X)} \left[\frac{d_x}{2} \log \frac{\mathbb{E}_{p(X, \hat{X})} [\|\hat{X} - X\|^2 | X = x]}{d_x} \right] \quad (36)$$

$$\leq \frac{d_x}{2} \log(2\pi e) + \frac{d_x}{2} \log \frac{\mathbb{E}_{x \sim p(X)} [\mathbb{E}_{p(X, \hat{X})} [\|\hat{X} - X\|^2 | X = x]]}{d_x} \quad (37)$$

$$= \frac{d_x}{2} \log(2\pi e) + \frac{d_x}{2} \log \frac{\mathbb{E}_{p(X, \hat{X})} [\|\hat{X} - X\|^2]}{d_x}. \quad (38)$$

The first inequality holds because the Gaussian distribution is the maximum entropy distribution among distributions with the same mean value and covariance. The second inequality depends on Lemma E.2. The Equation 36 holds because,

$$\text{tr}(\text{Cov}(\hat{X}|X = x)) = \sum_{i=1}^{d_x} \mathbb{E}_{p(\hat{X}_i)} [(\hat{X}_i - \mathbb{E}[\hat{X}_i])^2 | X = x], \quad (39)$$

where the mean vector $\mathbb{E}_{p(\hat{X}_i)} = X$ when the DRA adversary is unbiased, and the second-order norm of $(\hat{X} - X)$ is $\sqrt{\sum_{i=1}^{d_x} (\hat{X}_i - X_i)^2}$. The third inequality stems from Jensen's inequality, where for all concave functions f (e.g., log), $f(\mathbb{E}[x]) \geq \mathbb{E}[f(x)]$. Hence, we can have:

$$\frac{\mathbb{E}_{p(X, \hat{X})} [\|X - \hat{X}\|^2]}{d_x} \geq \frac{e^{\frac{2}{d_x} H(\hat{X}|X)}}{2\pi e}. \quad (40)$$

□

F. Proof of Theorem 4.4

First, we have the following Lemma:

Lemma F.1. (Theorem 9 in (Scarlett & Cevher, 2019)). Under the minimax estimation setup in Section 4.3, fix $\epsilon > 0$, and index $V \in \mathcal{V}$ is drawn from a prior distribution P_V . $X_V = \{x_{v_1}, \dots, x_{v_{|V|}}\}$ drawn from a probability distribution $P_{X|V}$ be a finite subset of \mathcal{X} such that

$$\rho(x_v, x_{v'}) \geq \epsilon, \forall v, v' \in \mathcal{V}, v \neq v'. \quad (41)$$

Then, we have

$$\mathcal{M}_n(\mathcal{X}, \ell) \geq \Phi\left(\frac{\epsilon}{2}\right)\left(1 - \frac{I(V; \hat{V}) + \log 2}{\log |\mathcal{V}|}\right), \quad (42)$$

where V is uniform on \mathcal{V} , and the mutual information is with respect to $V \rightarrow X_V \rightarrow Z \rightarrow \hat{X} \rightarrow \hat{V}$.

Proof. In Lemma F.1, the X_V is identified by V , so we let both V and X_V be the raw input X in split inference. In this case, given the $V = X$, we have $X_V = V = X$, where the X_V is uniquely identified by V . Then, we let Z be the smashed data Z and both \hat{X} and \hat{V} be the reconstructed input \hat{X} in split inference system, and we have the Markov chain

$$X \rightarrow X \rightarrow Z \rightarrow \hat{X} \rightarrow \hat{X}.$$

Follow (Noorbakhsh et al., 2024), we assume X is uniform over \mathcal{X} . Then by applying Lemma F.1 and using $I(X; \hat{X}) = H(\hat{X}) - H(\hat{X}|X)$, we reach out Theorem 4.4. \square